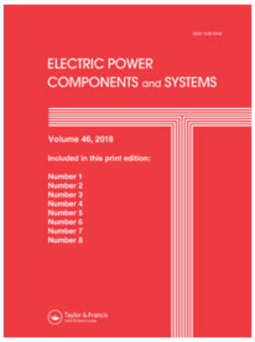

Electric Power Components and Systems

ISSN: 1532-5008 (Print) 1532-5016 (Online) Journal homepage: www.tandfonline.com/journals/uemp20

Enhanced Predictive Torque Control with Auto-Tuning Feature for Induction Motor Drive

Kodumur Meesala Ravi Eswar, Kunisetti Venkata Praveen Kumar & Thippiripati Vinay Kumar

Electric Power Components and Systems, 46(7): 825–836, 2018

ISSN: 1532-5008 print / 1532-5016 online
DOI: 10.1080/15325008.2018.1509157

Enhanced Predictive Torque Control with Auto-Tuning Feature for Induction Motor Drive

Kodumur Meesala Ravi Eswar, Kunisetti Venkata Praveen Kumar and Thippiripati Vinay Kumar
Electrical Engineering Department, National Institute of Technology, Warangal, India

CONTENTS

Abstract—This article presents an improved predictive torque control scheme for an induction motor (IM) drive by incorporating auto tuning feature. Among the variant control techniques, predictive torque control for an IM drive is the real choice for high dynamic performance and it became more popular since it involves control parameters in cost function. Weighting factor adjustment in cost function has direct influence in the performance of a drive. The main problem associated with the conventional predictive torque control scheme is the selection of convenient weighting factors to accomplish optimal torque and flux response. To overcome this problem, auto tuning of weighting factor based on control objective is introduced. With this, optimal weighting factor is selected for cost function evaluation in every sampling time, thereby giving desired performance. To validate this, MATLAB/Simulink and experimental results are presented for an IM drive fed by two level voltage source inverter. These results establish that proposed control scheme of IM drive exhibits optimal torque and flux response.

Keywords: auto tuning, induction motor (IM) drive, predictive torque control (PTC), voltage source inverter (VSI)
Received, 10 July 2017; accepted, 29 July 2018

Address correspondence to Kodumur Meesala Ravi Eswar, Electrical Engineering Department, National Institute of Technology, Warangal 506004, India. E-mail: nit.ravieswar@gmail.com

Color versions of one or more of the figures in the article can be found online at www.tandfonline.com/uemp.

1. INTRODUCTION

Induction motor (IM) drive became more popular for an industrial applications, owing to its advantages. Faster evolution of microprocessors, facilitates for emerging new control schemes for motor drive applications. These emerging techniques aimed to boost the overall performance of a motor drive.

In former 1960s, the first control method performed on IM is vector control [1,2]. The controlling is done in rotating frame of reference. The principle concept involved is alignment of direct-axis (d-axis) with the synchronously rotating rotor flux axis. With this, d-axis current component align with rotor flux and quadrature-axis (q-axis) current component align right angle to rotor flux. Thus, flux and torque controlling is made independent. This control makes to appear IM as an equivalent DC machine. Despite the advantages, this method has some negative points. One is torque control is via currents. Moreover, the control structure needs rotor flux observer for the estimation of rotor flux angle and current components. It also involves reference frame transformations and current regulators. These necessities hike computation complexity.

To alleviate the demerits of first control method, direct torque control (DTC) is introduced in the year 1986 [3]. This method executes control of drive in stationary reference frame. DTC comprises of two nonlinear hysteresis controllers. They are flux and torque hysteresis controllers. The inputs to these controllers are flux error and torque error, respectively. Flux hysteresis controller is of 2-level and torque hysteresis controller is of 3-level. The output of both the hysteresis controllers elects optimum switching states of inverter from the look-up table. Therefore by applying appropriate voltage vector there can be change in magnitude of stator flux along with the angle between stator and rotor flux. This has faster and direct influence on torque and flux of a machine. However, it has some demerits: large ripple in torque and flux, hysteresis controller implementation in digital platform requires large sample frequency, switching frequency dependent on hysteresis bands and motor speed. These problems are addressed in [4–7].

Nowadays, Predictive control scheme is the emerging technology [8–10]. Predictive control scheme can be made applicable for both converter and electric drive applications [11]. Owing to its advantages such as ease of practice, intuitive nature, and direct incorporation of control parameters; makes predictive control to create remarkable development in the control process. Predictive torque control (PTC) is one of the applications of predictive control scheme in electric drive applications. PTC scheme can be considered as alternative to DTC which is most emerging and successful control technique in electric drive applications [12]. PTC does not have non-linear hysteresis controllers and does not need heuristic lookup tables for voltage vector switchings as in the case of DTC. In PTC optimum voltage vector switching states are computed based on depreciation of cost function. In [13–15], Predictive control scheme is conducted for various converter configurations in the application of converters and drives.

The PTC scheme cost function may involve multi objective functions. It may be torque, flux, reactive power, common mode voltage, switching frequency. The structures of cost function for different control objective terms are represented in [16]. As the control objective terms are different, weighting factors need to be assigned to make relative balance among them. This weighting factor adjustment plays key role in the overall control performance of a drive. Several researches are going on for the selection of convenient weighting factor for the optimal control of a drive. In [16–19], predictive control is performed, where the weighting factor selection is based on empirical approach. In [20], predictive control based multi objective genetic algorithm for the optimization of weighting factor is introduced. In [21,22], optimal weight is determined, considering the derivative of torque ripple square with respect to weight is zero. However in [21,22], optimization of weighting factor is complex and depends on system parameters, obviously this is not advisable. In [23], predictive control is carried out by elimination of weighting factors. However, it leads to increase in computation burden with the increase in number of switching states. In [24,25], PTC of IM drive using fuzzy technique is introduced to address the weighting factor selection problem. In [26,27], PTC of IM drive is implemented using multi objective TOPSIS and VIKOR methods while addressing the weighting factor problem. In [28], PTC of IM is performed fed by 2-level VSI with empirical weighting factors in cost function while limiting prediction voltage vectors.

Aside from these elucidations presented in literature, this article proposes a simple online based optimal weighting factor selection for cost function evaluation. Unlike conventional PTC, where fixed weighting factor is selected in cost function, the proposed method results in improved performance, as the weight is self-tuned to an optimal values in each sample interval based on system variations. The proposed PTC of IM drive is verified by conducting MATLAB simulations and real time experimentation using dSPACE control board.

2. SYNTHESIS OF IM MODEL

The most well-known voltage and flux linkage space vector mathematical equations [29] for an IM in stationary reference frame are given as Eqs (1)–(4). The subscript 's' and 'r' signifies stator and rotor terms, respectively. The generated electromagnetic torque and motor-load torque equation are given as Eqs (5) and (6). The terms ω_m and ω_r represents motor mechanical and electrical speed.

$$V_s = R_s i_s + p\lambda_s \tag{1}$$

$$0 = R_r i_r + p\lambda_r - j\omega_r\lambda_r \tag{2}$$

$$\lambda_s = L_s i_s + L_m i_r \tag{3}$$

$$\lambda_r = L_r i_r + L_m i_s \tag{4}$$

$$T_{motor} = \frac{3}{2}\frac{P}{2}\left(imag\left(\bar{\lambda}_s i_s\right)\right) \tag{5}$$

$$T_{motor} - T_{load} = J\frac{d\omega_m}{dt} \tag{6}$$

These Equations (1)–(4) are represented in state space model considering i_s and λ_s terms as state variables. Thus the state space representation of machine model is as follows:

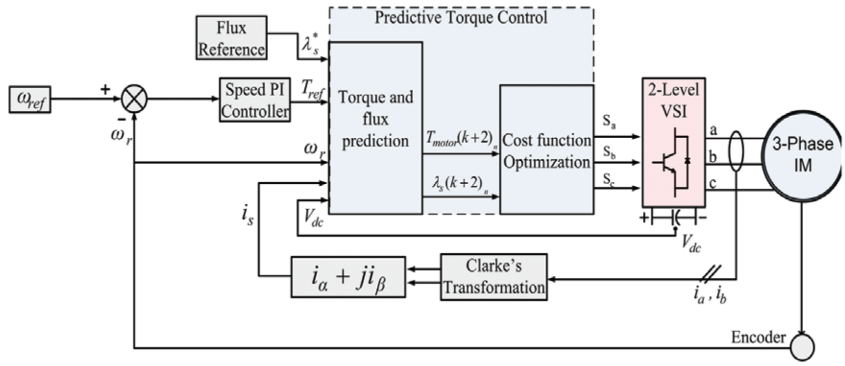

FIGURE 1. Conventional PTC for IM drive fed by 2-Level VSI.

$$\frac{di_s}{dt} = A_1\left(A_2\lambda_s - A_3 i_s + K_r(V_s - Ai_s - j\omega_r\lambda_s) + \frac{j\omega_r i_s}{A_1}\right) \tag{7}$$

$$\frac{d\lambda_s}{dt} = (V_s - Ai_s) \tag{8}$$

Where,

$$A = R_s \quad A_1 = \frac{L_m}{L_s L_r - L_m{}^2} \quad A_2 = \frac{R_r}{L_m} \quad A_3 = \frac{L_s R_r}{L_m} \tag{9}$$

$$K_r = \frac{L_r}{L_m} \quad p = \frac{d}{dt}$$

These Equations (7) and (8) are represented in discrete form in PTC algorithm.

3. BASIC PTC OF IM DRIVE

Figure 1 shows conventional PTC operational block diagram. Torque reference is obtained from speed PI controller. Motor speed (ω_r), measured current (i_s), torque reference (T_{ref}), and flux reference magnitude (λ_s*) are given to the PTC algorithm for controlling purpose and generation of switching pulses. PTC algorithm contains mathematical model of system in discrete form. This discretization is done using forward Euler method. The basic representation of it is given as:

$$\frac{dz}{dt} = \frac{z(k+1) - z(k)}{T_S} \tag{10}$$

Where, T_s is sampling time and z is any state variable.

3.1. Measurements

3.1.1. Stator flux estimation. Machine stator flux cannot be measured directly. Therefore, by using Euler mathematical analysis, stator flux has to be estimated. From Eq. (8), stator flux at present state (k) can be estimated as:

$$\lambda_s(k) = \lambda_s(k-1) + V_s T_s - AT_s i_s \tag{11}$$

3.1.2. Stator current measurement. Stator currents can be directly measured from motor terminals. The measured currents i_a, i_b, and i_c are converted to i_α and i_β using Clarke's transformation. From this, measured current space vector is obtained as:

$$i_s = i_\alpha + ji_\beta \tag{12}$$

3.1.3. Prediction. Stator flux, current, and torque need to be predicted. Prediction is done for all the available switching vectors relating to a given inverter. For a 2-level VSI, there are '8' possible switching vectors as represented in Table 1 in stationary reference frame.

Predicted flux, current and torque equations for one step ahead ($k+1$) are represented as:

$$(\lambda_s(k+1))_n = \lambda_s(k) + T_s\left((V_s)_n - Ai_s(k)\right) \tag{13}$$

$$i_s(k+1)_n = i_s(k) + T_s\left(A_1\left(A_2\lambda_s(k) - A_3 i_s(k) + K_r\left((V_s)_n - Ai_s(k) - j\omega_r\lambda_s(k)\right) + \frac{j\omega_r i_s(k)}{A_1}\right)\right) \tag{14}$$

$$(T_{motor}(k+1))_n = \frac{3}{2}\frac{P}{2}\left(imag\left(\bar{\lambda}_s(k+1)_n * i_s(k+1)_n\right)\right) \quad (15)$$

where: $n = (V_o, V_1, V_2 .... V_7)$

3.2. Cost function

Cost function is composed of multi-objective terms which have to be controlled. For all the switching states, predicted values of control parameters are compared with their reference values. The switching state which realizes predicted value closeness to reference value is selected as optimum. The basic representation of cost function with two control objectives (torque and flux) can be given as follows:

$$G_n = |T_{ref} - T_{motor}(k+1)_n| + W|\lambda_s{}^* - |\lambda_s(k+1)_n|| \quad (16)$$

Where, W is the flux weighting factor which signifies importance between torque and stator flux control objectives comparatively. The terms T_{ref} represents reference torque generated by speed PI controller and $\lambda_s{}^*$ is the reference stator flux magnitude.

The equations of torque, current, and flux predictions Eq. (13)–(15) represents one step ahead. Owing to the practical sample delay problems in the PTC algorithm [30], two step ahead prediction ($k+2$) is preferred. The modified equations can be expressed as:

$$(\lambda_s(k+2))_n = \lambda_s(k+1) + T_s\left((Vs)_n - Ai_s(k+1)\right) \quad (17)$$

$$i_s(k+2)_n = i_s(k+1) + T_s\left(A_1\left(A_2\lambda_s(k+1) - A_3 i_s(k+1) + K_r\left((V_s)_n - Ai_s(k+1) - j\omega_r\lambda_s(k+1)\right) + \frac{j\omega_r i_s(k+1)}{A_1}\right)\right) \quad (18)$$

$$(T_{motor}(k+2))_n = \frac{3}{2}\frac{P}{2}\left(imag\left(\bar{\lambda}_s(k+2)_n * i_s(k+2)_n\right)\right) \quad (19)$$

With the obtained two step predicted torque and flux Eqs (17)–(19), cost function can be reformulated and is given by Eq. (20):

$$G_n = |T_{ref} - T_{motor}(k+2)_n| + W|\lambda_s{}^* - |\lambda_s(k+2)_n|| \quad (20)$$

In [19,29], weighting factor is depicted as the ratio of nominal values of motor torque and flux. It is represented as:

Switching vectors (V_s)	(S_a,S_b,S_c)	V$_\alpha$	V$_\beta$
Vo	(0,0,0)	0	0
V1	(1,0,0)	0.66667Vdc	0
V2	(1,1,0)	0.3333Vdc	0.5773Vdc
V3	(0,1,0)	−0.3333Vdc	0.5773Vdc
V4	(0,1,1)	−0.66667Vdc	0
V5	(0,0,1)	−0.3333Vdc	−0.5773Vdc
V6	(1,0,1)	0.3333Vdc	−0.5773Vdc
V7	(1,1,1)	0	0

TABLE 1. Switching vectors for 2-Level VSI in stationary reference frame.

$$W = \frac{T_{nom}}{\lambda_{nom}} \quad (21)$$

This value of weighting factor (W) is considered only at initial point of time and it may vary in real time implementation for proper tuning.

4. PROPOSED PTC OF IM DRIVE

The paramount steps in PTC are: (1) Estimation of unknown variables, (2) Prediction of system behavior, and (3) Output optimization based on cost function minimization. Owing to the multiple control objectives in single cost function (toque and flux), weighting factor has direct impact on selection of optimal voltage vector and thereby control performance of motor drive. Figure 2 represents block diagram of proposed PTC for IM drive fed by 2-level VSI. In this weighting factor is tuned to an optimum value for every sampling time. This tuned value of weighting factor is applied in cost function to obtain optimal control response. Pictorial representation of this control process is shown in Figure 3.

Consider an objective function (flux) for which the weighting factor is assigned. From cost function (20) it is given as:

$$K = |\lambda_s{}^* - |\lambda_s(k+2)_n|| \leq G_{opt} \quad (22)$$

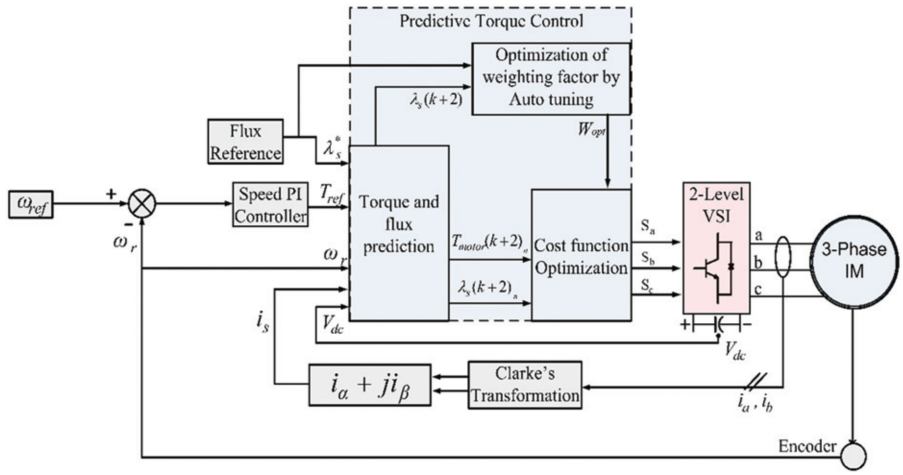

FIGURE 2. Block diagram of proposed PTC.

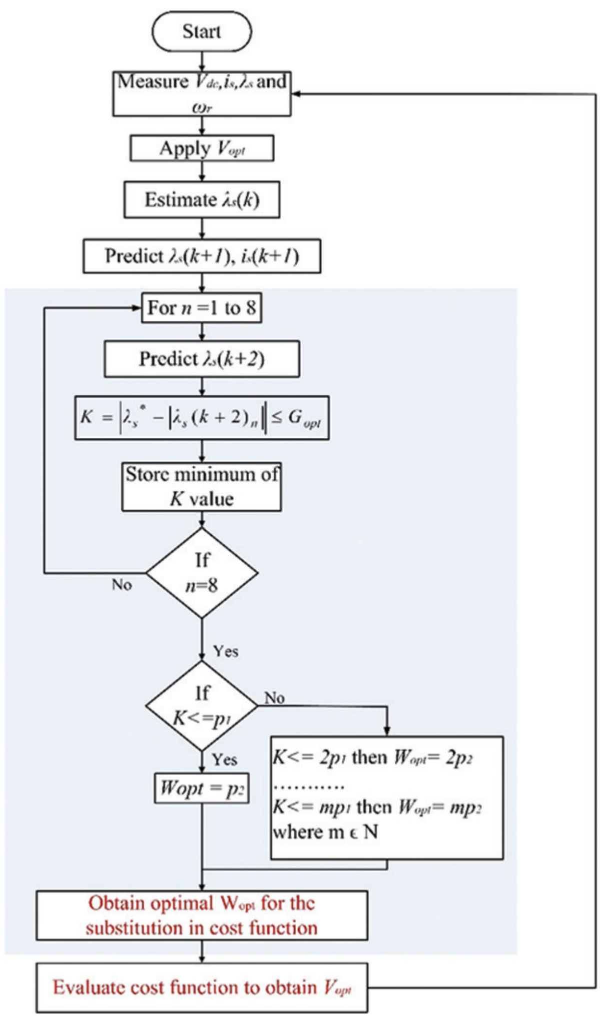

FIGURE 3. Proposed PTC flowchart.

where, G_{opt} is the flux error. The flux error value is set to 0.08 Wb.

For all the '8' switching states, 'K' is computed and minimum of 'K' value is selected. Variables 'p_1' and 'p_2' are selected as considerably small numbers to minimize torque and flux ripples. Here 'p_1' value is set to 0.05 which is maximum permissible flux ripple and 'p_2' value is set to 5 which is multiplication factor for the flux weighting factor (W_{opt}). If the minimum value of 'K' is less than or equal to 'p_1', optimal weighting factor is selected as Eq. (24). It indicates that the flux response is in permissible level while increasing the contribution of torque control objective in cost function thereby reduction in torque ripple.

$$\text{Minimum } (K) <= p_1 \tag{23}$$

$$W_{opt} = p_2 \tag{24}$$

If the above condition (23) is not satisfied, it implies that flux ripple is more. Then it checks for the condition (25).

$$\text{Minimum } (K) <= mp_1 \tag{25}$$

If this condition (25) is satisfied, then optimal weighting factor is set to,

$$W_{opt} = mp_2 \tag{26}$$

Where 'm' belongs to natural numbers set (N). In this auto-tuning process, the natural number set is considered till the value of 15. As the value of 'p_2' is set to 5, the maximum tuned weighting factor value is 75.

It means that, if the flux control objective function minimum value does not satisfy the constraint (23), it checks the condition (25) for every value of N. With the satisfaction of condition (25), weighting factor increases its magnitude by multiplying 'm' times with 'p_2' as shown in Eq. (26). Therefore increase in the value of W_{opt} results in increasing the contribution of flux control objective in cost function and thereby reduction in flux ripples. The optimum value of weighting factor (W_{opt}) is substituted in cost function as shown in Eq. (27).

This process repeats for every sample interval. With this system, optimization is done online and optimal value of W_{opt} is selected in every sample period based on flux control objective. The modified cost function with the optimized tuned weight is given by Eq. (27) and it is assessed for all the eight switching states of inverter. The switching state providing minimum cost function value is selected for switching in next sample interval. This auto-tuning feature helps in the selection of optimal voltage vector (V_{opt}) to enhance the motor torque and flux response achieving minimum torque and flux ripples.

$$G_n = |T_{ref} - T_{motor}(k+2)_n| + W_{opt}|\lambda_s{}^* - |\lambda_s(k+2)_n|| \tag{27}$$

5. RESULTS AND DISCUSSIONS

5.1. Simulation results

To verify the proposed control strategy as shown in Figure 2, IM is modeled using mathematical Equations (1)–(6) in MATLAB/Simulink environment. The real time machine parameters are tabulated as shown in Table 2. To compare the effectiveness of proposed model, both conventional and proposed PTC are performed on IM drive. Simulations are configured with the sampling time $T_s = 50\ \mu s$.

Name	Notation	Value
Stator resistance	R_s	1.8 Ω
Rotor resistance	R_r	0.8 Ω
Stator inductance	L_s	0.54 H
Rotor inductance	L_r	0.54 H
Mutual inductance	L_m	0.512 H
Poles	P	4
Inertia	J	0.031 kg-m^2
Rated power	P_n	3.7 kW
Rated speed	N_r	1440 RPM
Rated torque	T_n	24.5 Nm
Rated line-line voltage	V_{LL}	415 V

TABLE 2. Existing IM specifications.

Inverter DC link voltage is considered as 540 V. The machine flux reference magnitude is set to 1 Wb. For comparing proposed PTC simulation results with the conventional, a conventional weighting factor is selected empirically in conventional PTC and its value is fixed to 70. While in the proposed PTC of IM drive, optimum weighting factor is selected in every sampling interval automatically with the incorporation of auto tuning feature.

At first steady state behavior of machine is analyzed in comparison with the conventional model. Figure 4 illustrates the steady state behavior of machine at reference electrical speed of 200 rad/sec till the simulation time 3 sec exhibiting forward motoring operation. A step change in reference speed of -200 rad/sec is triggered at the time instant 3 sec. Thus the motor exhibited dynamic characteristics from the instant 3 sec to 3.25 sec is analyzed. After the time instant of 3.25 sec, motor starts rotating in reverse direction, thus exhibiting reverse motoring characteristics. Figure 4 represents the characteristics of motor speed, torque, flux, phase voltage, and current under various operating conditions of reference speeds at no-load. From these results, it is conveyed that the proposed PTC of IM drive exhibits optimal steady state torque and flux response when compared with the conventional PTC scheme. Both these schemes exhibits similar dynamic response during the step changes in motor reference speed.

Now the IM drive is operated at the rated reference electrical speed (301 rad/sec) and full load torque

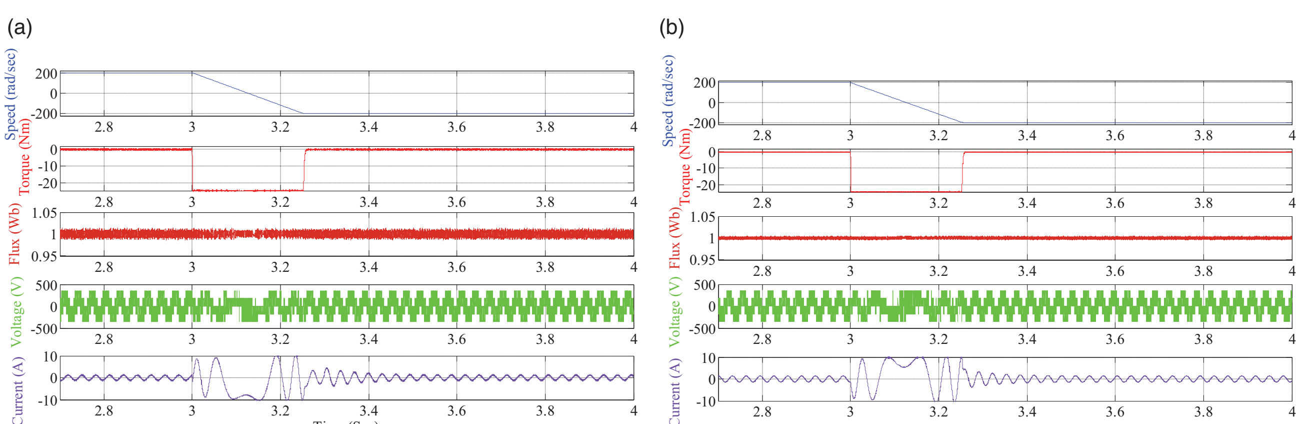

FIGURE 4. Motor speed, torque, flux, phase voltage, and current characteristics. (a) Conventional PTC of IM drive and (b) Proposed PTC of IM drive.

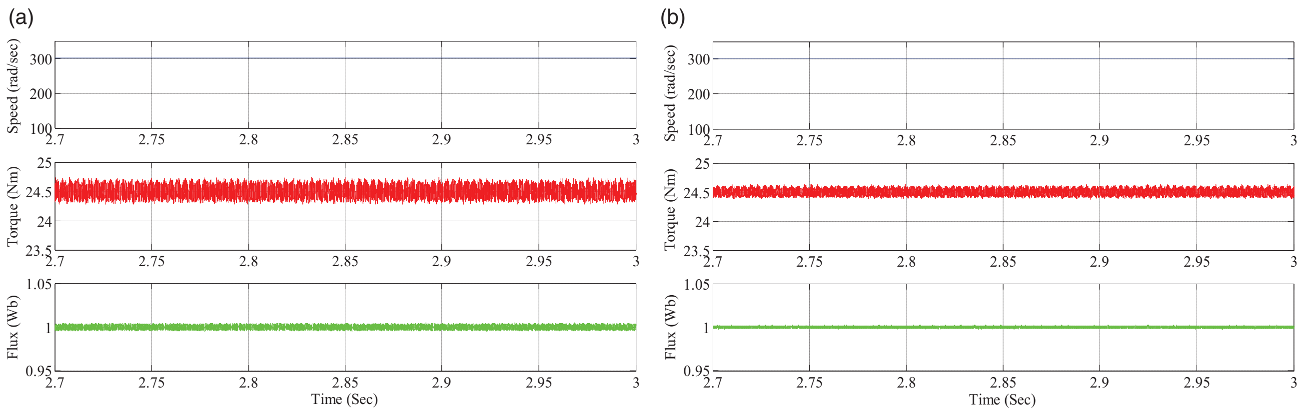

FIGURE 5. Motor speed, torque, and flux steady state characteristics. (a) Conventional PTC of IM drive and (b) Proposed PTC of IM drive

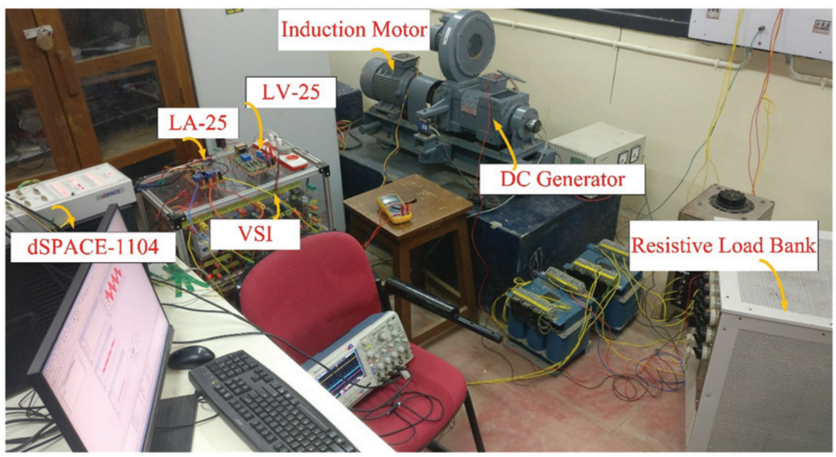

FIGURE 6. Test bench setup of IM drive with dSPACE 1104.

(24.5 Nm) conditions. The exhibited motor speed, torque and flux steady state characteristics are shown in Figure 5.

From the above all results, it has been shown that the online based optimization of weighting factor results in overall better performance of motor torque and flux in comparison with the conventional PTC of IM drive.

5.2. Hardware results

To validate the proposed PTC of IM drive practically, experimentation is performed on 5 HP, 1440 RPM IM drive fed by 2-level VSI. The machine parameters are displayed in Table 2. The experimental test rig of IM drive is presented in Figure 6. The proposed PTC algorithm is programed in dSPACE (RTI 1104) platform with the sampling time of 50 μs. The motor speed is measured using Encoder and interfaced to dSPACE incremental encoder. The IM drive phase currents and voltage are measured using current sensors (LA-25) and voltage sensor (LV-25), respectively. Thus, the required measurements are sensed and fed to predictive control algorithm with the help of dSPACE ADC BNC connectors. Based on the cost function minimization, switching pulses are generated for the 2-level VSI. These pulses are collected from the digital I/O connectors of dSPACE controller board and interfaced to inverter switches.

Experimental results of proposed PTC are exhibited in Figures 7–11 in comparison with the conventional PTC of IM drive, to validate its effectiveness. The steady state speed, motor torque, phase voltage, and current characteristics under the reference speed of 250 rad/sec and load torque of 14 Nm are exhibited in Figure 7. It is observed that the motor torque response is improved for the proposed PTC in comparison with the conventional scheme. In conventional PTC, with the adjustment of weighting factor by trial and error method, better results can be obtained,

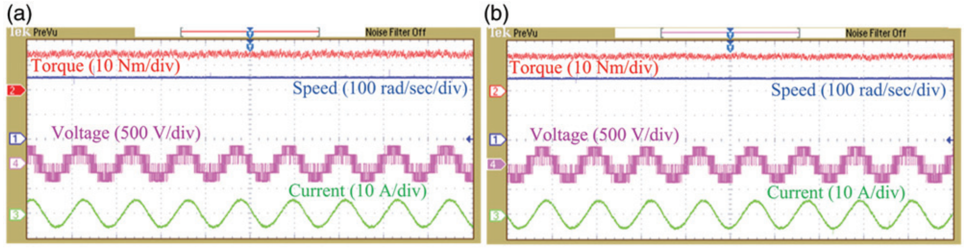

FIGURE 7. Steady state motor speed, torque, current, and voltage for reference speed 250 rad/sec and load torque 14 Nm. (a) Conventional PTC (b) Proposed PTC. (X-axis time scale—20 ms/div).

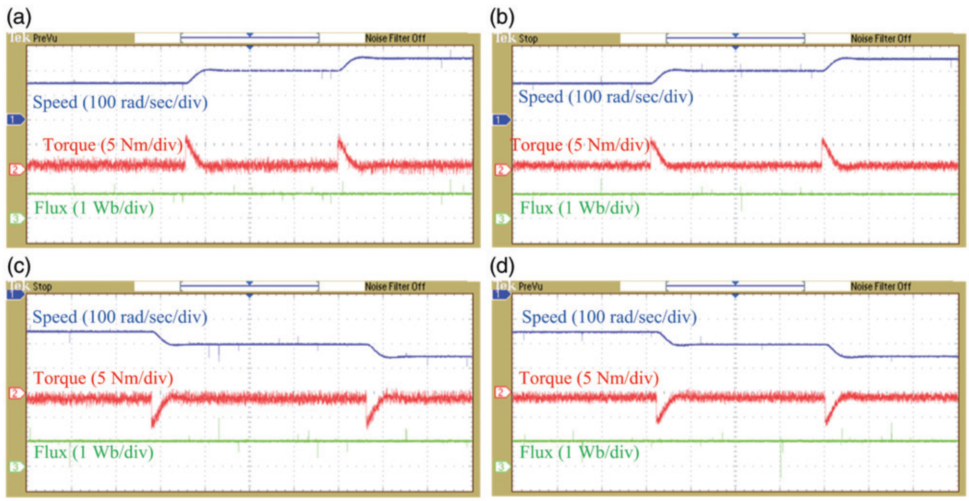

FIGURE 8. Motor speed, torque, and flux characteristics with change in reference speed. For forward motoring (a) in conventional PTC and (b) in Proposed PTC. For reverse motoring (c) in conventional PTC and (d) in Proposed PTC. (X-axis time scale—1 sec/div)

where as in proposed PTC, weighting factor is auto tuned and optimal value is selected for the better control response of IM drive.

To analyze the motor response for step changes in reference speed, dSPACE controlDesk software is used for the provision of instant step changes in motor reference speed. To verify the dynamic response of IM drive, step change in reference speed of IM is set from 150 to 200 rad/sec and then 200 to 250 rad/sec at no load. Its related motor speed, torque, and flux characteristics are shown in Figure 8a and 8b for the conventional and proposed PTC of IM drive respectively. These results represent forward motoring. The same can be verified in reverse motoring, i.e., from −150 to −200 rad/sec and then −200 to −250 rad/sec. Its respective motor speed, torque, and flux characteristics are shown in Figure 8c and 8d for the conventional and proposed PTC of IM drive, respectively. From these results it can be verified that the proposed PTC of IM drive exhibits better steady state torque and flux response having low ripples when compared to conventional scheme.

A step change in reference speed is given from forward motoring at 200 rad/sec to reverse motoring at −200 rad/sec. The response of torque, flux, and motor phase current along with its speed are shown in Figure 9a and 9b for the conventional and proposed PTC of IM drive, respectively.

From these results, it can be observed that both of the schemes of IM drive exhibits similar dynamic characteristics with improved steady state performance in proposed scheme. To examine the performance of conventional and proposed PTC of IM drive under load disturbance conditions, IM is coupled to DC generator. By loading DC generator with a resistive load bank, step changes in motor load torque are performed while motor is operating at speed of 200 rad/sec. Its motor speed, torque, current, and flux characteristics are shown in Figure 10a and 10b for the conventional and proposed PTC of IM drive for step change in load torque from no load to 12.25 Nm (50% load).

Figure 10c and 10d represents motor steady state speed, torque, current, and flux characteristics at 50% of

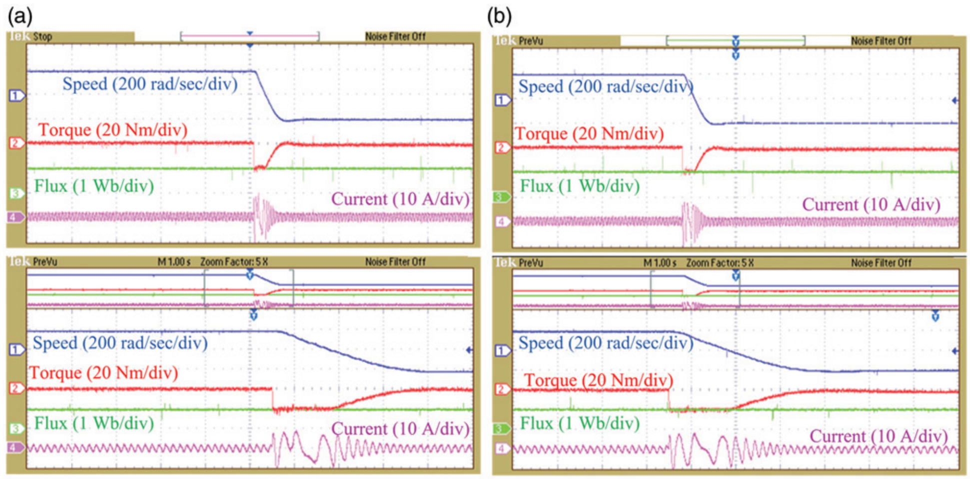

FIGURE 9. Motor speed, torque, flux and current characteristics with change in reference speed from forward to reverse. (a) In conventional PTC and (b) in Proposed PTC. (X-axis time scale—1 sec/div)

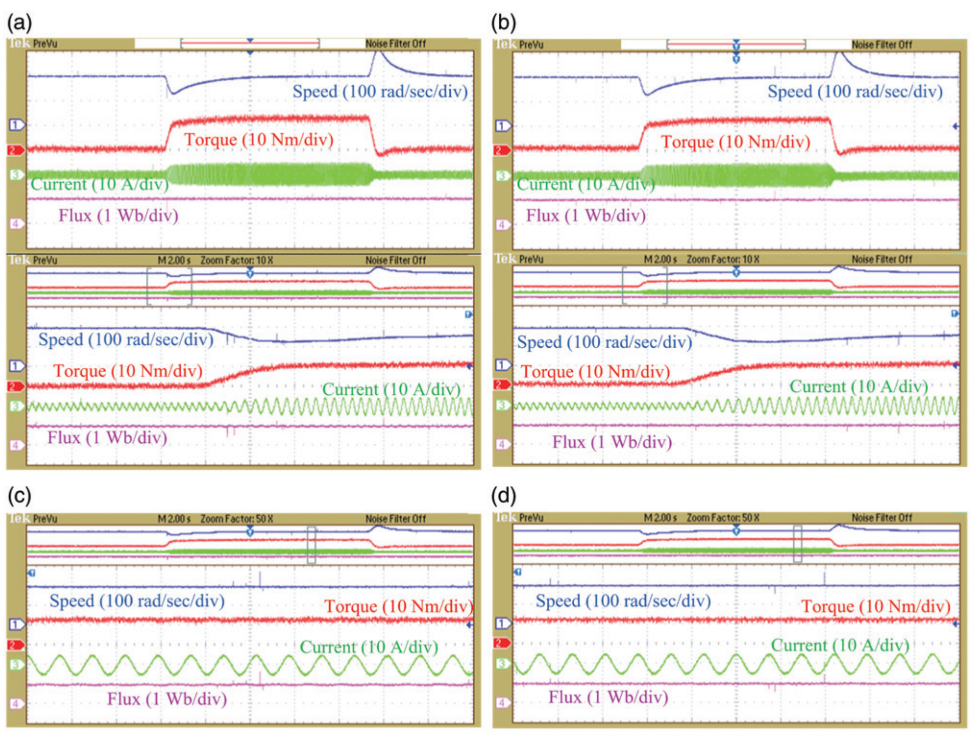

FIGURE 10. Motor speed, torque, flux and current characteristics with step changes in load torque. (a) and (c) conventional PTC, (b) and (d) Proposed PTC. (X-axis time scale – 2sec/div)

motor load torque for the conventional and proposed PTC of IM drive. These results convey improved steady state performance of motor torque and flux for the proposed PTC. Both of these results convey similar dynamic response. Finally testing is done for conventional and proposed PTC of IM drive at rated electrical speed (301 rad/sec) and full load torque (24.5 Nm) condition. Its results are shown in Figure 11.

The motor torque and flux are measured for 125,000 samples. From the above conducted results of conventional and proposed PTC of IM drive, the average torque and flux ripples are evaluated considering the sum of the difference between the measured and reference values over 125,000 samples. The comparison table is prepared to show the effectiveness of proposed PTC over conventional PTC and DTC scheme of IM drive and are listed in Table 3. The

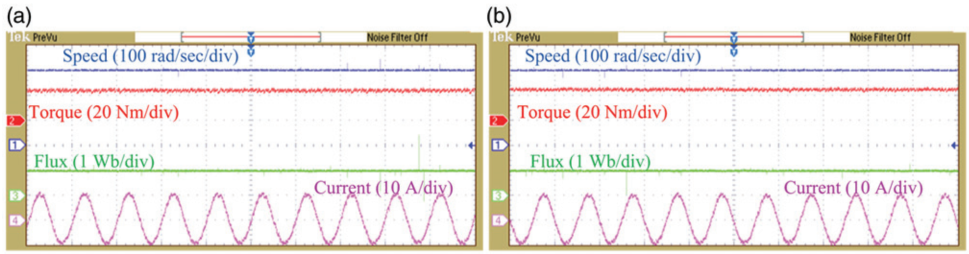

FIGURE 11. Motor speed, torque, flux and current characteristics. (a) Conventional PTC and (b) proposed PTC (X-axis time scale—20 ms/div).

Control scheme	Speed (Electrical)	Torque ripple (N-m)	Flux ripple (Wb)
DTC	150 rad/sec	2.75	0.064
Conventional PTC		1.82	0.032
Proposed PTC		1.64	0.026
DTC	200 rad/sec	2.45	0.058
Conventional PTC		1.601	0.028
Proposed PTC		1.42	0.016
DTC	250 rad/sec	2.32	0.044
Conventional PTC		1.28	0.014
Proposed PTC		1.20	0.012

TABLE 3. Comparison Table under various operating conditions of speed at no-load.

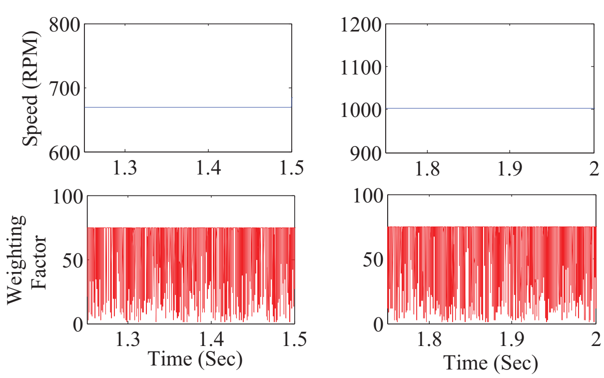

FIGURE 12. Weighting factor tuning.

characteristics of weighting factor tuning in proposed PTC for the electrical speeds 140 rad/sec (mechanical—668.4 RPM) and 210 rad/sec (mechanical—1002.6 RPM) are shown in Figure 12. The weighting factor tuning in each sample interval is observed till the value of 75.

At motor rated speed and full load torque condition as shown in Figure 11, the average motor torque and flux ripple achieved in conventional PTC of IM drive are 1.18 Nm and 0.012 Wb. Whereas for the proposed PTC, the achieved average torque and flux ripple values are 1.16 Nm and 0.011 Wb, respectively.

The average computation time for the conventional PTC is 20.25 µs and for the proposed PTC with the involvement of auto-tuning feature, the computation time increased to 28.5 µs. However, it is a good solution for better response of motor drive because the weighting factor is auto-tuned and leads to optimal control response. Finally, it is validated that the auto tuning of flux weighting factor (W_{opt}) facilitates an improved steady state performance of torque and flux of IM drive while implementing proposed PTC.

6. CONCLUSION

The selection of weighting factor and its adjustment is the main troublesome in PTC execution. This article presents a simple auto tuning based weighting factor selection for IM drive fed by 2-level VSI. The proposed feature enables optimization of weighting factor in every sampling time. This optimization is based on minimization of control objective function. The cost function is formulated with the optimized weight factor and optimal switching states are selected while minimizing the cost function.

The proposed PTC strategy is verified with the both simulation and experimentation on IM drive. The obtained steady state motor torque and flux characteristics under various operating conditions demonstrates the improved performance of IM drive without any manual tuning as in the case of conventional PTC. In addition, the proposed PTC exhibits similar dynamic characteristics to that of conventional scheme. Finally, an effective and simple application of torque and flux control of IM drive with the proposed PTC scheme is possible.

ORCID

Kodumur Meesala Ravi Eswar http://orcid.org/0000-0002-6724-008X
Kunisetti Venkata Praveen Kumar http://orcid.org/0000-0001-7384-961X
Thippiripati Vinay Kumar http://orcid.org/0000-0002-7250-6655

REFERENCES

[1] F. Blaschke, "The principle of field-orientation as applied to the TRANSVECTOR closed-loop control system for rotating-field machines," *Siemens Rev.*, vol. 34, pp. 217–220, 1972.
[2] S. Sathikumar, and J. Vithayathil, "Digital simulation of field-oriented control of induction motor," *IEEE Trans. Indus. Electron.*, vol. IE-31, no. 2, pp. 141–148, 1984.
[3] I. Takahashi, and T. Noguchi, "A new quick-response and high-efficiency control of an induction motor," *IEEE Trans. Indus. Appl.*, vol. IA-22, no. 5, pp. 820–827, 1986.
[4] L. Kyo-Beum, S. Joong-Ho, C. Ick, and Y. Ji-Yoon, "Torque ripple reduction in DTC of induction motor driven by three-level inverter with low switching frequency," *IEEE Trans. Power Electron.*, vol. 11, pp. 255–264, 2002.
[5] K.-K. Shyu, J.-K. Lin, V.-T. Pham, M.-J. Yang, and T.-W. Wang, "Global minimum torque ripple design for direct torque control of induction motor drives," *IEEE Trans. Ind. Electron*, vol. 57, no. 9, pp. 3148–3156, Sep. 2010.
[6] R. Ramchand, K. Gopakumar, C. Patel, K. Sivakumar, A. Das, and H. Abu-Rub, "Online computation of hysteresis boundary for constant switching frequency current-error space-vector-based hysteresis controller for VSI fed IM drives," *IEEE Trans. Power Electron.*, vol. 27, no. 3, pp. 1521–1529, Mar. 2012.
[7] T. V. Kumar, and S. S. Rao, "Hardware implementation of direct load angle controlled induction motor drive," *Electr. Power Component Syst.*, vol. 42, no. 14, pp. 1505–1516, 2014.
[8] J. Maciejowski, *Predictive Control with Constraints*, New York: Prentice-Hall, 2002.
[9] E. Camacho, and C. Bordons, *Model Predictive Control*, Berlin, Germany: Springer-Verlag, 2007.
[10] J. Rawlings, and D. Mayne, *Model Predictive Control, Theory and Design*. Madison, WI: Nob Hill Publ., 2009.
[11] A. Linder, and R. Kennel, "Model predictive control for electrical drives," presented at Power Electronics Specialists Conference, 2005. PESC '05. IEEE 36th, 2005, pp. 1793–1799.
[12] F. Wang, Z. Zhang, R. Kennel, and J. Rodríguez, "Model predictive torque control with an extended prediction horizon for electrical drive systems", *Int. J. Control.*, vol. 88, no. 7, pp. 1379–1388, 2015.
[13] V. Yaramasu, M. Rivera, M. Narimani, B. Wu, and J. Rodriguez, "Finite state model based predictive current control with two-step horizon for four-leg NPC converters," *J. Power Electron*, vol. 14, no. 6, pp. 1178–1188, 2014.
[14] D. Zhou, J. Zhao, and Y. Liu, "Predictive torque control scheme for three-phase four-switch inverter-fed induction motor drives with DC link voltages offset suppression", *IEEE Trans. Power Electron.*, vol. 30, no. 6, pp. 3309–3318, 2015.
[15] D. Zhou, J. Zhao, and Y. Li, "Model predictive control scheme of five leg AC-DC-AC converter-fed induction motor drive," *IEEE Trans. Ind. Electron*, vol. 63, no. 7, pp. 4517–4526, 2016.
[16] P. Cortes, *et al.*, "Guidelines for weighting factors design in model predictive control of power converters and drives," presented at Proc. IEEE Int. Conf. Ind. Technol. (ICIT'09), 2009, pp. 17.
[17] J. Rodriguez *et al.*, "State of the art of finite control set model predictive control in power electronics," *IEEE Trans. Ind. Inf*, vol. 9, no. 2, pp. 1003–1016, May 2013.
[18] R. Vargas, U. Ammann, B. Hudoffsky, J. Rodriguez, and P. Wheeler, "Predictive torque control of an induction machine fed by a matrix converter with reactive input power control," *IEEE Trans. Power Electron*, vol. 25, no. 6, pp. 1426–1438, Jun. 2010.
[19] J. Rodriguez, R. M. Kennel, J. R. Espinoza, M. Trincado, C. A. Silva, and C. A. Rojas, "High-performance control strategies for electrical drives: An experimental assessment," *IEEE Trans. Ind. Electron*, vol. 59, no. 2, pp. 812–820, Feb. 2012.
[20] P. Zanchetta, "Heuristic Multi-Objective optimization for cost function weights selection in finite state model predictive control", workshop on predictive control of electrical drives and power electronics," PRECEDE, 2011.
[21] S. A. Davari, D. A. Khaburi, and R. Kennel, "An improved FCS-MPC algorithm for induction motor with imposed optimized weighting factor," *IEEE Trans. Power Electron.*, vol. 27, no. 3, pp. 1540–1551, 2011.
[22] M. Uddin, S. Mekhilef, M. Mubin, M. Rivera, and J. Rodriguez, "Model predictive torque ripple reduction with weighting factor optimization fed by an indirect matrix converter," *Electr. Power Component Syst.*, vol. 42, no. 10, pp. 1059–1069, 2014.
[23] C. A. Rojas, J. Rodriguez, F. Villarroel, J. R. Espinoza, C. A. Silva, and M. Trincado, "Predictive torque and flux control without weighting factors," *IEEE Trans. Ind. Electron*, vol. 60, no. 2, pp. 681–690, Feb. 2013.
[24] D. Zhou, J. Zaho, and Y. Liu, "Online tuning of weighting factors based on sugeno-fuzzy method in predictive torque control of four switch three-phase inverter-fed IM," presented at Int. Symp. on Power Electronics, Electrical Drives, Automation and Motion, pp. 734–739, 2016.
[25] C. A. Rojas, S. Kouro, and M. Perez, "Multiobjective fuzzy predictive torque control of an induction machine fed by a 3L-NPC inverter", presented at Proc. 2015 IEEE int. Symp. on predictive control of electrical drives and power electronics," October, pp. 21–26, 2015.
[26] V. P. Muddineni, S. R. Sandepudi, and A. K. Bonala, "Finite control set predictive torque control for induction motor drive with simplified weighting factor selection using

TOPSIS method", *IET Electric Power Appl*., vol. 11, no. 5, pp. 749–760, 2017.

[27] V. P. Muddineni, A. K. Bonala, and S. R. Sandepudi, "Enhanced weighting factor selection for predictive torque control of induction motor drive based on VIKOR method", *IET Electric Power Appl*., vol. 10, no. 9, pp. 877–888, 2016.

[28] M. Habibullah, D. D. C. Lu, D. Xiao, and M. F. Rahman, "A simplified Finite-State predictive direct torque control for induction motor drive", *IEEE Trans. Indus. Electron*., vol. 63, no. 6, pp. 3964–3975, June 2016.

[29] R. Jose, and C. Patricio, *Predictive Control of Power Converters and Electrical Drives*, Hoboken, NJ: John Wiley & Sons, 2012.

[30] P. Cortes, J. Rodriguez, C. Silva, and A. Flores, "Delay compensation in model predictive current control of a three-phase inverter," in *IEEE Trans. Indus. Electron*., vol. 59, no. 2, pp. 1323–1325, Feb. 2012.

BIOGRAPHIES

Kodumur Meesala Ravi Eswar received his B.Tech degree in Electrical and Electronics Engineering from Jawaharlal Nehru Technological University, Ananthapur, India, in 2014 and M.Tech degree from VIT University, Vellore, India, in 2016. Presently he is doing research in the area of Power Electronics and Drives at National Institute of Technology, Warangal, India.

Kunisetti Venkata Praveen Kumar received his B.Tech degree in Electrical and Electronics Engineering from Jawaharlal Nehru Technological University, Kakinada, India, in 2011 and M.Tech degree from JNTU, Kakinada, India, in 2014. Presently he is doing research in the area of Power Electronics and Drives at National Institute of Technology, Warangal, India.

Thippiripati Vinay Kumar received his B.Tech degree in Electrical and Electronics Engineering from Jawaharlal Nehru Technological University, Hyderabad, India, in 2005 and M.Tech degree from JNTU, Hyderabad, India, in 2008. He received his Ph.D degree from National Institute of Technology, Warangal, India, in 2014. Since 2013, he is working as an assistant professor in National Institute of Technology, Warangal, India. He published many research papers in national and international journals and conferences. His research interests are power electronics and drives, multi-level inverters and renewable energy.